EXPERIMENTAL EVALUATION OF SCALE EFFECT ON PLASTIC DEFORMATION CAPACITY OF STEEL BEAM-END CONNECTION

S. Kishiki[1], T. Kawabata[2], T. Nakagomi[3], Y. Murata[4], S. Aoyagi[5], K. Kasai[6]

[1] *Associate Professor, Tokyo Institute of Technology, kishiki.s.aa@m.titech.ac.jp*
[2] *Professor, The University of Tokyo, kawabata@fract.t.u-tokyo.ac.jp*
[3] *Professor Emeritus, Shinshu University, nakagom@shinshu-u.ac.jp*
[4] *Graduate Student, Shinshu University, 18w5029c@shinshu-u.ac.jp*
[5] *Former Graduate Student, Tokyo Institute of Technology, aoyagi.hs9.satoshi@jp.nipponsteel.com*
[6] Special Appointed Professor, Tokyo Institute of Technology, kasai.k.ac@m.titech.ac.jp

Abstract

In high-rise steel buildings, size of structural members tends to be larger and higher strength steel has been also developed to reduce its weight. Although seismic performances of high-rise buildings are evaluated by numerical analysis based on structural behavior and plastic deformation capacity, its assumptions have not been proved by real scale experiments. It means that most of experiments have employed the scaled specimens because of limitation of experiment facilities.

However, it has long been said that in steel structure, the risk of brittle fracture increases as the plate thickness of steel material increases, and this is called "Scale Effect". In fact, in beam members, a beam flange is an important factor causing brittle fracture, and the large-section member used for a high-rise building may not exhibit the plastic deformation capacity expected in design. In addition, although some studies on the scale effect have been conducted since the Kobe Earthquake in 1995, there are few studies on the scale effect of beam-end connection where sufficient plastic deformation capacity is expected in seismic design, and the influence is not fully known.

Therefore, this paper describes experimental evaluation of the scale effect on plastic deformation capacity of the beam-end connection. The specimen is a simple beam including beam to column connection, and the main parameter is the "(a) specimen size". There are three types of specimen sizes: full size, 1/2 scale and 1/4 scale. In addition to the main parameters, there are two sub-parameters "(b) connection details", and "(c) artificial weld defects".

Experimental results showed that the plastic deformation capacity tended to decrease as the flange thickness increased, although material toughness of the full-size specimen is the largest among them. It means that the scale effect on the beam-end connection is confirmed from this comparison. And, from the experimental results on connection details, it was confirmed that the connection detail greatly affected the plastic deformation capacity of the beam-end connection. In particular, when the weld access hole was made small extremely, the hole toe was close to the welded part of the beam flange, and it may promote strain concentration and significantly reduce the plastic deformation performance of the beam-end connection. Also, from the other results with weld defects on full penetration weld, it was proved that allowable defect size in Japan was enough to consider the scale effect on decrease of plastic deformation capacity.

Keywords: steel structure, beam-end connection, brittle fracture, scale effect

1. Introduction

In the 1995 Kobe earthquake, failures at beam-end connections of steel structures were reported, and studies on the causes of brittle fractures and studies on securing plastic deformation capacity have been conducted. On the other hand, as buildings become taller in recent years, large-section members have often been used for steel buildings, but it has been reported before the Kobe earthquake that brittle fracture is more likely to occur as the plate thickness increases [1]. Large-section members may not exhibit the plastic deformation capacity expected in design.

Therefore, in order to verify the safety of such members, an experiment using full-size specimens is necessary, but in reality, many experiments using scaled-specimens are conducted due to limitation on experimental facilities in Japan. As a study on the scale effect, Kuwamura et al.[2] conducted experiments of the effects of material toughness and flange thickness, however there are few studies on scale effect of steel beam-end connections.

Therefore, in this study, three-point bending experiments are conducted on the beam specimens with the various scale, and it experimentally verified the influence of the scale effect at the beam-end connection. In this paper, three series of experimental results as a study of the scale effect at the beam-end connections are reported.

(a) "Specimen size"

: An experiment on the beams whose member dimensions are roughly scaled in three stages of 1: 1/2: 1/4 based on the beam cross section of BH-1200×500×25×40.

(b) "Connection details"

: An experiment using parameters such as the shape of a weld access hole and the distance from the hole toe to the welded part of the beam flange as the details of the connection.

(c) "Weld defects"

: An experiment in which the artificial weld defect size is scaled in addition to the beam specimen size.

2. Overview of beam specimen

2.1 Shape of beam specimen

A shape of each beam specimen is shown in Fig.1. The beam specimen is a weld built-up H-shaped cross section, and the dimensions of the members are roughly scaled in three stages of 1: 1/2: 1/4 (Hereafter, L size, M size, S size respectively) based on BH-1200 × 500 × 25 × 40 and span of 5.5 m. The experiments were conducted by a simple beam subjected to a three-point bending method. A column with an H-shaped cross section is placed at the center of the specimen, and fulcrums at both ends are provided with horizontal roller jigs and connected via a joint part to a beam specimen.

At the beam end connection to the center column, both the flange and the web are welded. The beam webs of high-rise buildings in Japan are high-strength bolted joints via shear plates. However, it was difficult to scale the joint strength for each member size, therefore a welded joint with a clear scaled strength was adopted.

In addition, in the vicinity of the beam end, two vertical stiffeners of the same thickness to the web are provided at the two places to avoid local buckling. The shape of weld access hole is a compound circle with a radius $R1$ and a quarter of the radius $R2$ ($<R1$). The shape is basically the same regardless of the member size, which is widely used after the 1995 Kobe earthquake.
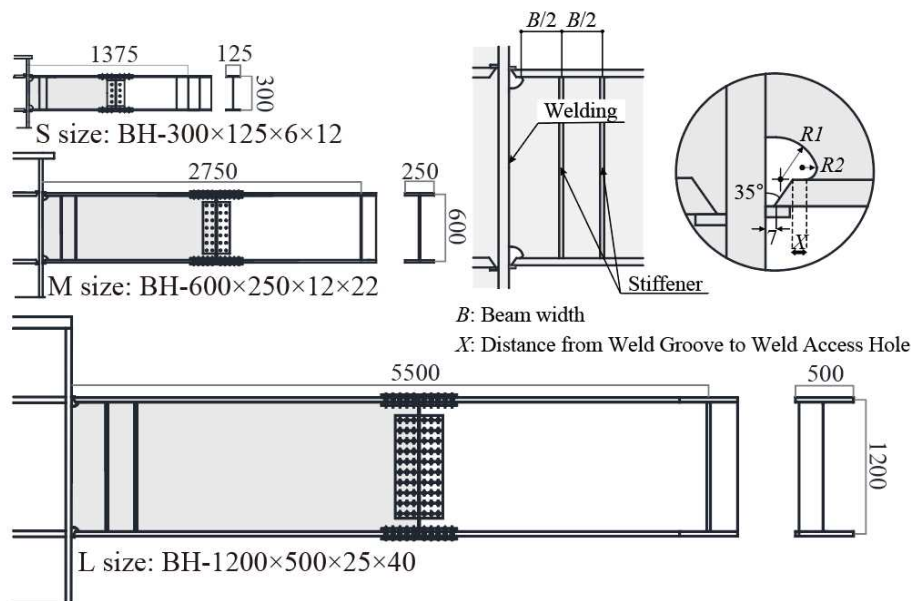

Fig.1 Outline of beam specimens

2.2 Specimen list

A list of beam specimens is shown in Table 1. The specimens consist of three specimens for "(a) specimen size", two specimens for "(b) connection details", and five specimens for "(c) artificial welding defects", for a total of ten specimens. The details of the weld defect will be described later.

Table 1   List of beam specimens

Specimen			L_b	X	Weld Access Hole Shape		Weld Defect
Parameters	Specimen Name	Beam Cross Section	[mm]	[mm]	$R1$ [mm]	$R2$ [mm]	
(1)	S_N	BH-300×125×6×12	1375	10	35	10	-
	M_N	BH-600×250×12×22	2750				
	L_N	BH-1200×500×25×40	5500				
(2)	S_SW	BH-300×125×6×12	1375	5	17.5	5	
	M_X15	BH-600×250×12×22	2750	15	35	10	
(3)	S_WD1	BH-300×125×6×12	1375	10	35	10	SD1
	M_WD1	BH-600×250×12×22	2750				MD1
	M_WD2	BH-600×250×12×22	2750				MD2
	L_WD1	BH-1200×500×25×40	5500				LD1
	L_WD2	BH-1200×500×25×40	5500				LD2

X: Distance from weld groove to weld access hole toe, *R1&R2*: Described in Fig. 1.

2.3 Mechanical properties and beam end joint performance

A chemical composition and mechanical properties of the steel used for the specimen are shown in Table 2 and 3, respectivly. And the structural properties of the beam-end connection are shown in Table 4. The steel material used for the beam flange was SN490B, however its toughness was adjusted as low as possible for the purpose of the experiment. In other words, the Charpy absorbed energy $_vE_0$ at 0 °C is 35 J for S size, 17 J for M size, and 112 J for L size. On the other hand, these chemical components and mechanical properties other than $_vE_0$ are almost the same value .

Table 2 Chemical composition of steel plate

Thickness	Chemical Composition[%]												Carbon Equivalent
[mm]	C	Si	Mn	P	S	Cu	Ni	Cr	Mo	Nb	V	B	C_{eq}[%]
12	0.13	0.23	1.30	0.013	0.004	0.11	0.06	0.10	0.02	0.012	0.003	0.0001	0.38
22	0.14	0.22	1.28	0.018	0.005	0.15	0.09	0.14	0.03	0.012	0.002	0.0002	0.40
40	0.14	0.22	1.28	0.018	0.005	0.15	0.09	0.14	0.03	0.012	0.002	0.0002	0.40

Table 3 Material properties of beam flange

Specimen	Steel Grade	Norminal Thickness	Yield Point	Tensile Strength	Yield Ratio	Elongation	$_vE_0$
		[mm]	[N/mm^2]	[N/mm^2]	[%]	[%]	[J]
Flange	SN490B	12	360.5	546.3	66.0	25.4	35
		22	341.0	552.8	61.7	27.4	17
		40	352.6	546.2	64.5	30.0	112

3

Table 4 Structural properties of each beam specimen

Size	Beam section	$_bM_p$ [kN·m]	K_c [kNm/rad]	$_b\delta_p$ [mm]	$_b\theta_p$ [rad]
S	BH-300×125×6×12	204	27907	9.87	0.00731
M	BH-600×250×12×22	1418	208844	18.68	0.00679
L	BH-1200×500×25×40	11220	1592618	38.75	0.00704

$_bM_p$:Full plastic moment, K_c: Elastic modulus,

$_b\delta_p$:Elastic deformation corresponding to $_bM_p$, $_b\theta_p$ Elastic angle corresponding to $_bM_p$

3. Experimental outline

Setup of an L-size specimen as an example of the specimen is illustrated in Fig.2. A three-point bending method was employed to conducted experiments of the simply beam. The loading protocol shown in Fig.3 is based on the elastic member angle $_b\theta_p$ corresponding to the full plastic moment, and the incremental displacement amplitude is 2 $_b\theta_p$.
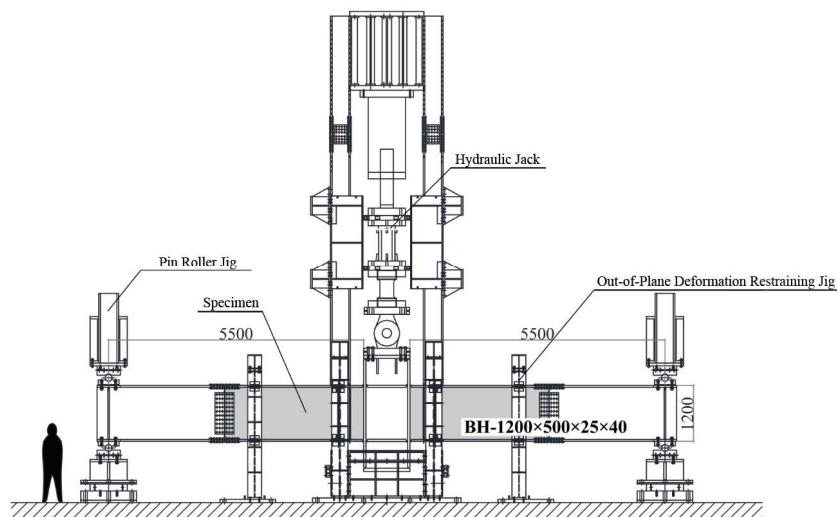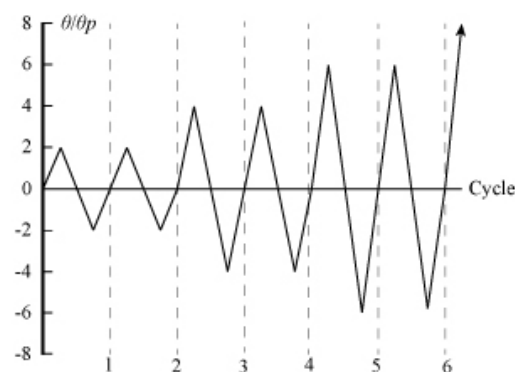

Fig.2 Experiment set-up of L size specimen

Fig.3 Loading protocol

4. Evaluation method of plastic deformation capacity

In this paper, the plastic deformation ratio $_E\eta_s$ in the skeleton curve defined by equation (1) is used to evaluate the plastic deformation capacity of the beam. Here, W_s is the absorbed energy shown in the Fig.4, $_bM_p$ is a full plastic moment of beam, and $_b\theta_p$ is an elastic angle corresponding to $_bM_p$. The skeleton curve was extracted by connecting the skeleton parts of the hysteresis curve obtained from the results of the loading experiment, as shown in Fig.4.

$$_E\eta_s = \frac{W_s}{_bM_p \cdot _b\theta_p} \tag{1}$$
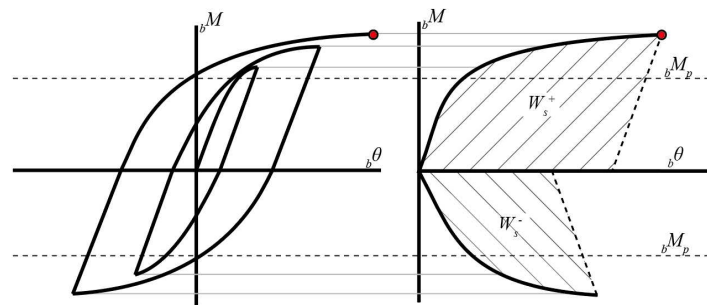
Fig.4 Extraction of skeletal curve

5. Experiment with specimen size as a parameter

5.1 Overview

Specimens whose parameters are member dimensions are S_N, M_N, and L_N shown in Table 5. The specimen size is generally scaled in three stages of 1: 1/2: 1/4 based on the beam cross section of BH-1200×500×25×40.

Table 5 List of scaled specimens

Specimen			L_b	X	Weld Access Hole Shape	
Parameters	Specimen Name	Beam Cross Section	[mm]	[mm]	$R1$ [mm]	$R2$ [mm]
(a)	S_N	BH-300×125×6×12	1375	10	35	10
	M_N	BH-600×250×12×22	2750			
	L_N	BH-1200×500×25×40	5500			

L_b:Beam span, X: Distance from weld groove to weld access hole toe

5.2 Experimental result

The experimental results are summarized in Table 6. In all the beam specimens, cracks were initially appeared from the toe of weld access hole, and it grew to brittle fracture of the beam flange. The hysteresis curves are compared in Fig.5. The vertical axis in the figure is the bending moment $_bM$ at the beam end, and the horizontal axis is the beam rotation angle $_b\theta$. The vertical axis is normalized by the full plastic moment $_bM_p$. The red dashed line in the figure is the calculated value of elastic stiffness and the full plastic moment. The symbol ● in the figure indicates the point at which the beam flange brittlely fractured. The hysteresis curves show almost the same shape, although they have different scale.

5

Table 6 Experimental result of scaled specimens

| Specimen Name | Equivalent Plastic Deformation Ration | | | Break cycle | Destructive Properties | Temperature |
	$_E\eta_s{}^+$	$_E\eta_s{}^-$	$_E\eta_s$			[°C]
S_N	7.7	5.5	13.2	5cycle(+5.83bθp)	Upper Flange Weld Access Hole Bottom	7～11
M_N	7.2	6.1	13.3	5cycle(+5.08$_b\theta_p$)	Upper Flange Weld Access Hole Bottom	13～14
L_N	5.2	6.0	11.2	5cycle(+2.07bθp)	Upper Flange Weld Access Hole Bottom	12～14
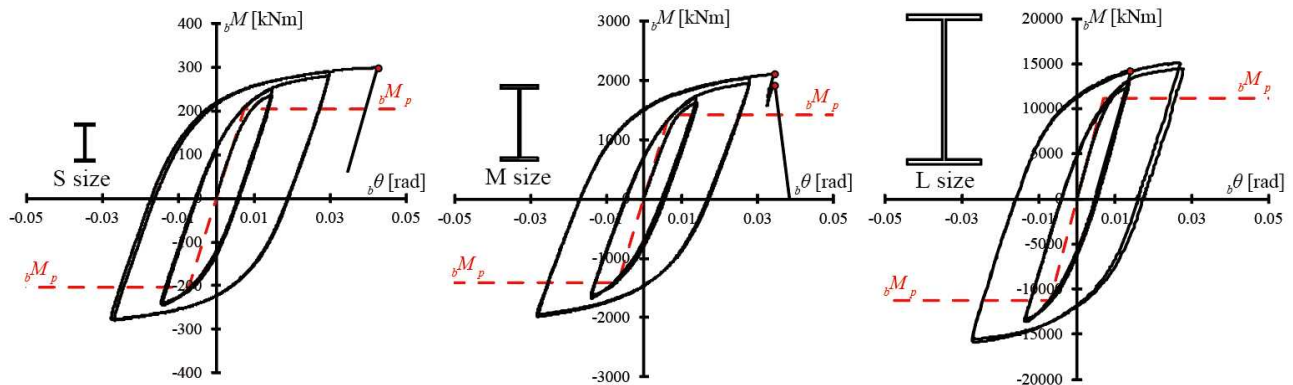
Fig.5 Hysteresis curve of scaled specimens

5. 3 Effect of member dimensions on deformation performance

Relationship between the thickness of the beam flange which is a representative value of the member dimensions, and the plastic deformation ratio $_E\eta_S$ which is an index of the plastic deformation capacity is shown in Fig.6. $_E\eta_S$ decreases as the member size increases, and it can be confirmed that the plastic deformation capacity decreases due to the scale effect, especially considering that the toughness of the L size is higher than the others.
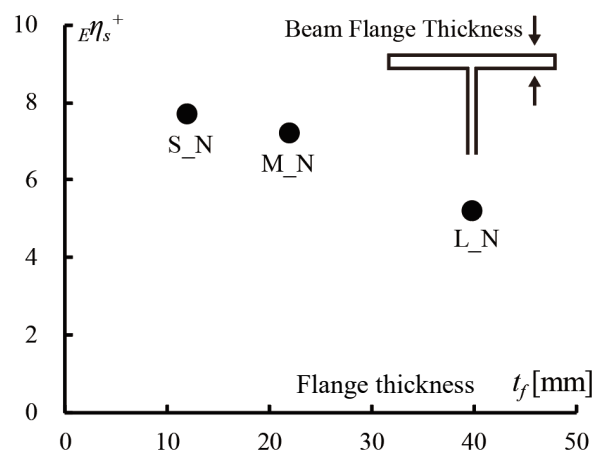

Fig.6 Effect of plate thickness on deformation capacity

6. Experiment with connection details as a parameter

6. 1 Overview

M_X15 and S_SW are specimens that have parameters of the connection detail in addition to the member dimensions shown in Table 7. Specimen M_X15 is a specimen whose distance from the weld groove to the

6

weld access hole toe (hereinafter referred to as distance X, Fig.7) is 15 mm. If this distance X is short, the weld part of full penetration welding and the weld access hole toe will be close to each other. It causes a strain concentration, so it is recommended that the distance X be set to about 10 mm in Japan. In the three specimens described above, while the distance X was 10 mm, the effect of the distance X on the deformation performance will be verified by setting the distance X of M_X15 to 15 mm.

Specimen S_SW, on the other hand, is a specimen in which the member dimensions, distance X, and the size of weld access hole are scaled to approximately half those of specimen M_N. In other words, based on the specimen M_N , not only the dimensions of the members but also the effect of scaling the connection details at the beam-end by half will be confirmed.

Table 7 List of specimen with scaled connection details

Specimen			L_b	X	Weld Access Hole Shape	
Parameters	Specimen Name	Beam Cross Section	[mm]	[mm]	$R1$ [mm]	$R2$ [mm]
(a)	S_N	BH-300×125×6×12	1375	10	35	10
	M_N	BH-600×250×12×22	2750			
(b)	S_SW	BH-300×125×6×12	1375	5	17.5	5
	M_X15	BH-600×250×12×22	2750	15	35	10
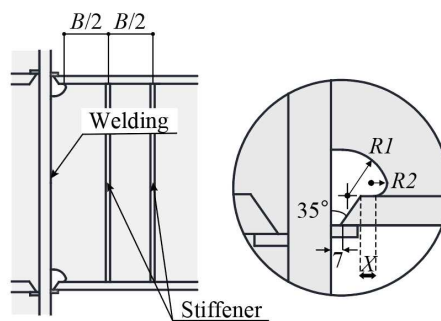
B: Beam width
X: Distance from Weld Groove to Weld Access Hole

Fig.7 Connection detail

6.2 Experimental result

A list of the experimental results is shown in Table 8, and hysteresis curves obtained from the experiment are compared in Fig.8. Similar to the three specimens described above, also in these two specimens, ductile cracks initially appeared at the toe of weld access hole, and grew up to the brittle fracture of the beam flange. In addition, the fracture occurred in the middle of the fifth cycle of the loading history shown in Fig.3.

Table 8 Experimental result of specimens with scaled connection details

| Specimen Name	Equivalent Plastic Deformation Ration			Break cycle	Destructive Properties	Temperature
	${}_E\eta_s{}^+$	${}_E\eta_s{}^-$	${}_E\eta_s$			[°C]
S_N	7.7	5.5	13.2	5cycle(+5.83bθp)	Upper Flange Weld Access Hole Bottom	7～11
M_N	7.2	6.1	13.3	5cycle(+5.08bθp)	Upper Flange Weld Access Hole Bottom	13～14
S_SW	5.0	5.6	10.6	5cycle(+3.92bθp)	Upper Flange Weld Access Hole Bottom	8～10
M_X15	8.8	8.3	17.1	5cycle(-4.57bθp)	Bottom Flange Weld Access Hole Bottom	11～12

7
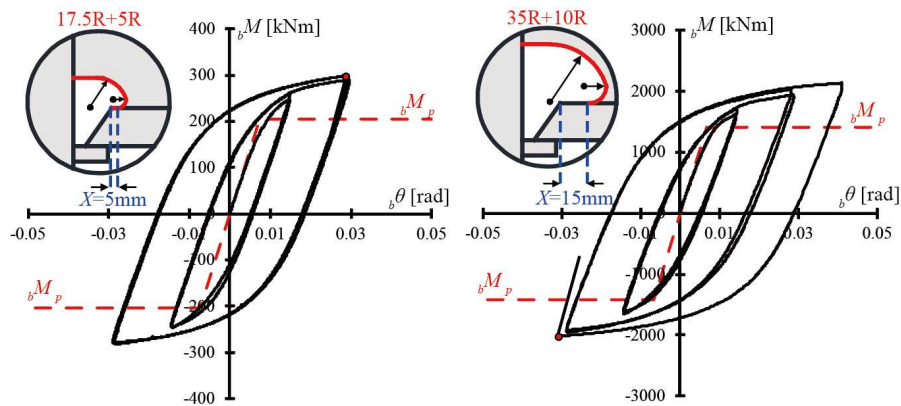
Fig.8 Hysteresis curve of specimens with scaled connection details

6.3 Influence of dimensions of joint details on deformation performance

As in the case of the beam specimen described above, the deformation capacity is evaluated by the equivalent plastic deformation ratio $_E\eta_S$, and the results are shown in Fig.9. From this evaluation, it can be confirmed that as the distance X becomes longer, the plastic deformation capacity up to the brittle fracture increases. However, if the distance X increases, it is considered that the plastic deformation capacity cannot be simply increased with respect to the horizontal axis due to the influence of secondary bending at the beam flange.
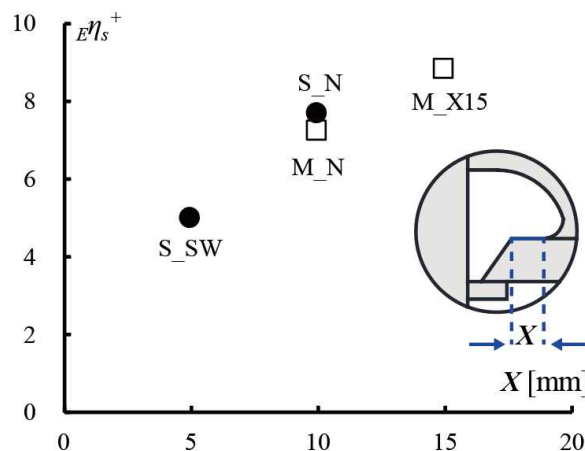
Fig.9 Effect of the connection detail on deformation capacity

7. Experiment with weld defects as a parameter

7. 1 Overview

Correspondence between specimen names and weld defects is shown in Table 9. And the size of the weld defect and the defect insertion position is illustrated in Fig.10. The artificial weld defects are assumed that an unwelded defect exists such as poor fusion at the beam flange side groove in the complete penetration weld of the beam flange. The unwelded defect was reproduced by inserting a steel plate in advance at the weld toe (center of the beam) near the bottom of the weld access hole, and the optimum steel plate shape was determined in advance through examination by welding tests.

8

It broadly classified the type of weld defect into two series. In the D1 series, the defect height was unified to 4.8 mm, which is about one pass of welding, and the defect length in the plate width direction was based on Architectural Institute of Japan (AIJ) standard [4], which was the boundary value of the defect evaluation length area ML. On the other hand, the D2 series is based on the S1 size defect (SD1) of the D1 series, and scales the defect size in the length direction and depth direction according to the ratio of the thickness of the beam flange.

Table 9 List of specimens with weld defect

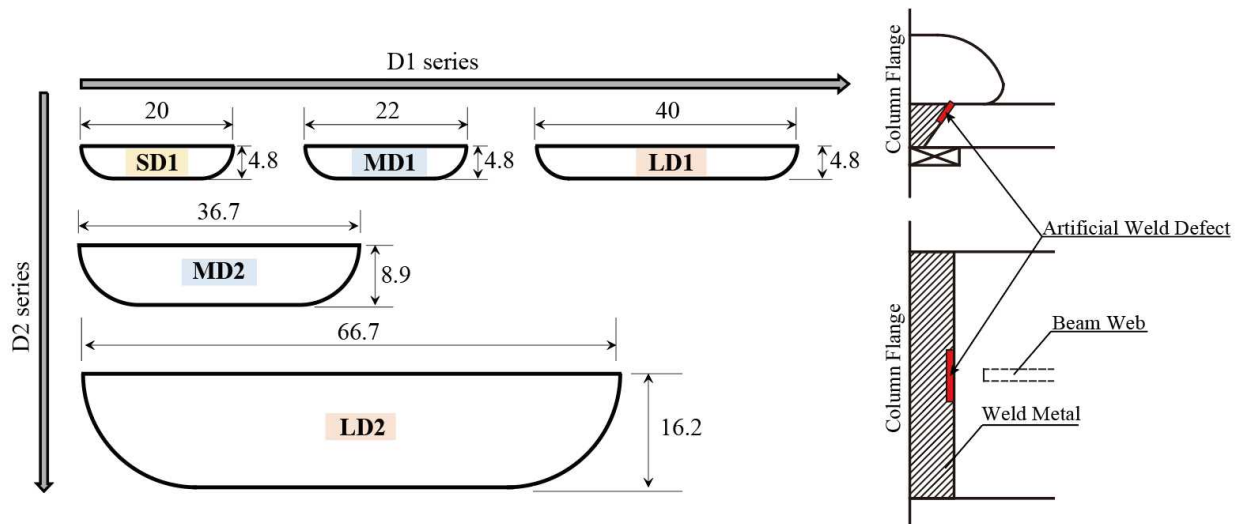| Specimen			L_b	X	Weld Access Hole Shape		Weld Defect
Parameters	Specimen Name	Beam Cross Section	[mm]	[mm]	$R1$ [mm]	$R2$ [mm]	
(3)	S_WD1	BH-300×125×6×12	1375	10	35	10	SD1
	M_WD1	BH-600×250×12×22	2750				MD1
	M_WD2	BH-600×250×12×22	2750				MD2
	L_WD1	BH-1200×500×25×40	5500				LD1
	L_WD2	BH-1200×500×25×40	5500				LD2

Fig.10 Outline of weld defect

7.2 Experimental result

The experimental results of the specimens with artificial weld defects are summarized in Table 10. And the hysteresis curves and the ultimate state of fracture section are shown in Fig.11 and 12, respectively. The specimens L_WD1, M_WD2, and L_WD2 led to brittle fracture from the artificial weld defect. On the other hand, for specimens S_WD1 and M_WD1, cracks propagated from the toe of weld access hole and led to brittle fracture. The fracture cycle of the specimens other than L_WD2 resulted in a 6 $_b\theta_p$ cycle, and only L_WD2 fractured in a 4 $_b\theta_p$ cycle.

Table10 Experimental result of specimens with weld defect

Specimen Name	Equivalent Plastic Deformation Ration			Break cycle	Destructive Properties	Temperature
	$_E\eta_s{}^+$	$_E\eta_s{}^-$	$_E\eta_s$			[°C]
S_WD1	5.5	5.7	11.2	5cycle(+4.04bθp)	Upper Flange Weld Access Hole Bottom	6
M_WD1	8.5	5.7	14.2	5cycle(-1.60$_b\theta_p$)	Bottom Flange Weld Access Hole Bottom	12〜14
L_WD1	8.5	11.8	20.3	6cycle(+3.53bθp)	Upper Flange Weld Defect	6〜11
M_WD2	3.3	1.6	4.9	5cycle(+4.73bθp)	Upper Flange Weld Defect	14〜16
L_WD2	6.7	6.1	12.8	3cycle(-0.43bθp)	Bottom Flange Weld Defect	14〜15

9

Fig.11 Hysteresis curve of specimens with weld defect

(a)S_WD1   (b)M_WD1   (c)L_WD1   (d)M_WD2   (e)L_WD2
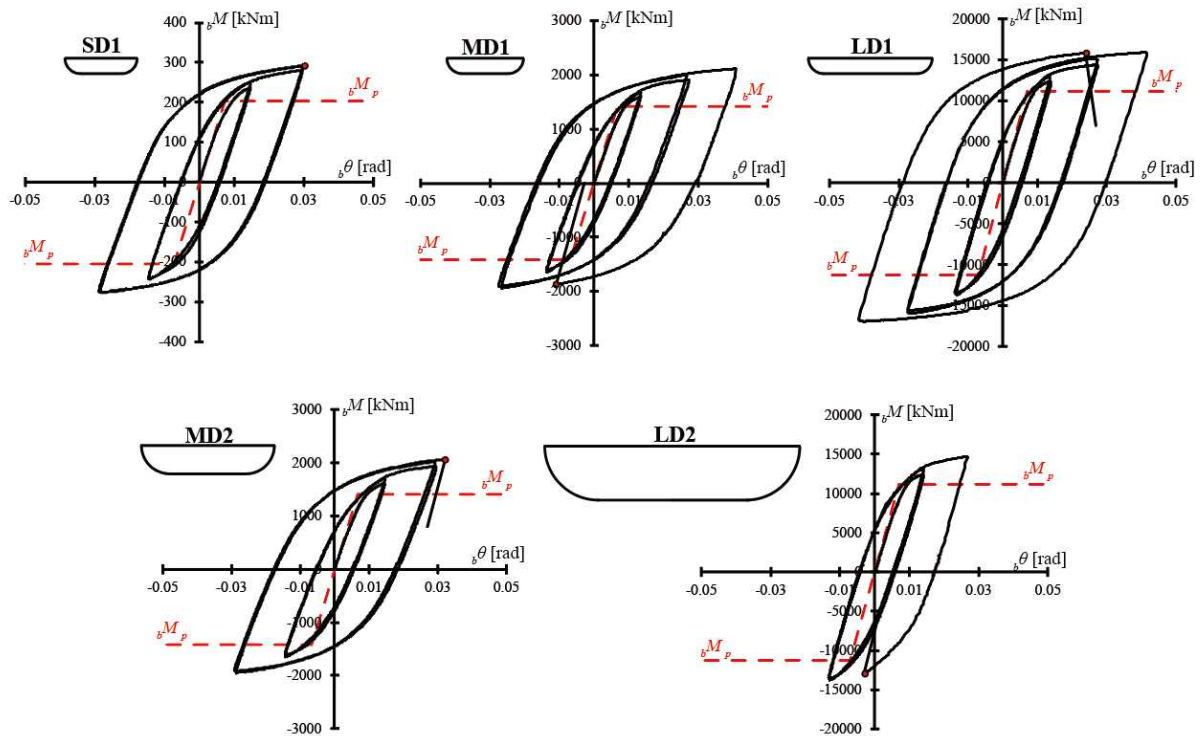
Fig.12 Ultimate state of fracture section of each specimen

7.3 Plastic deformation capacity

7.3.1 Weld defect WD1 series

The deformation performances of the WD1 series are compared in Fig.13. Unlike the result of the two parameters mentioned above, the larger the thickness of the beam flange, the greater the plastic deformation capability. For example, L_WD1 has about twice the plastic deformation capacity of S_WD1. This is considered to be due to the fact that plastic deformation occurred near the weld defect and delayed the initiation and propagation of cracks at the bottom of weld access hole.

From the crack growth at the bottom of weld access hole using the M size as an example in Fig.14, it can be seen that crack initiation and propagation at the bottom is slower in M_WD1 than in M_N.
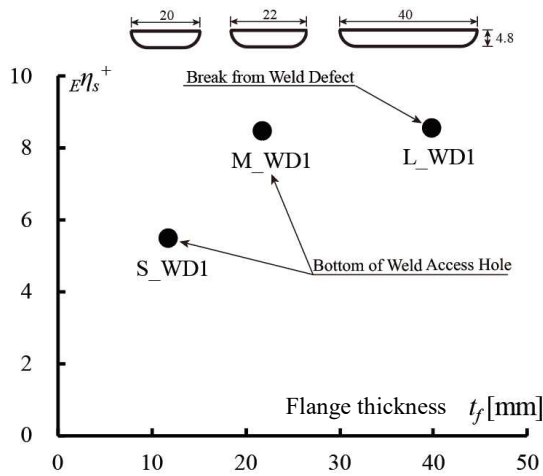
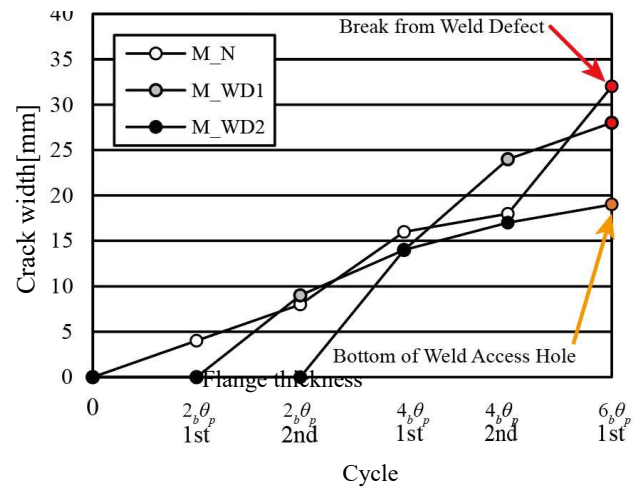Fig.13 Effect of weld defect D1 on deformation capacity

Fig.14 Crack growth process

7.3.2 Weld defect WD2 series

The deformation performances of the WD2 series are compared in Fig.15. In the WD2 series, S_WD1 and M_WD2 exhibited the same level of plastic deformation capacity, while L_WD2 exhibited only about 1/2 the other one. All specimens of the D1 series broke from the toe of weld access hole, while both specimens of the D2 series fractured from welding defects. From this result, it is considered that the depth of the welding defect has a greater effect on the plastic deformation capacity of the base material than the width.
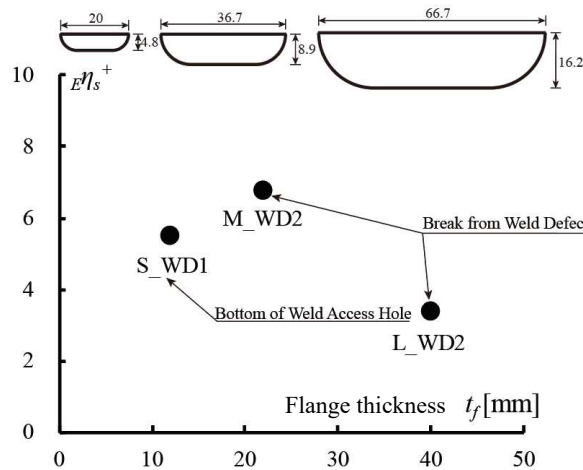

Fig.15 Effect of weld defect D2 on deformation capacity

8. Conclusion

As a verification experiment on the scale effect of the beam-end connection, a three-point bending test of a simple beam specimen was conducted with beam specimens scaled in three stages based on a cross section of BH-1200×500×25×40. From the experimental results with the specimen size as a parameter, the plastic deformation capacity tended to decrease as the flange thickness increased, although material toughness of full-scale specimen is the largest among them. It means that the scale effect on the beam-end connection is confirmed from the comparison.

11

From the experimental results with the connection details as a parameter, it was confirmed that the connection detail greatly affected the plastic deformation performance of the beam-end connection. In particular, when the weld access hole was made small extremely, the hole toe was close to the welded part of the beam flange, and it may promote strain concentration and significantly reduce the plastic deformation performance of the beam-end connection.

From the experimental results with the artificial weld defects as a parameter, it was proved that allowable defect size in AIJ standard was enough to consider the scale effect on decrease of plastic deformation capacity.

9. Acknowledgements

10. References

[1] Kato, B. and Morita, K., Brittle fracture of extremely thick members, J. Struct. Constr. Eng., AIJ, No.156(1969), pp.1-10 (in Japanese)

[2] Kuwamura,H. et al., Effects of material toughness and plate thickness on brittle fracture of steel members, J. Struct. Constr. Eng., AIJ, No.525(1999), pp.109-116, (in Japanese)

[3] uilding Research Institution, JISF(the Japan Iron and Steel Foundation) : Testing Methods of the Evaluation of Structural Performance for the Steel Structures,(2002),(in Japanese)

[4] Standard for the ultrasonic inspection of weld defects in steel structures AIJ (Architectural Institute of Japan) (1996) "Standard for Ultrasonic Inspection of Weld Defects in Steel Structures". (in Japanese)